Chinese Chemical Letters 35 (2024) 109030

Contents lists available at ScienceDirect

Chinese Chemical Letters

journal homepage: www.elsevier.com/locate/cclet

Rapid discovery of two unprecedented meroterpenoids from *Daphne altaica* Pall. using molecular networking integrated with MolNetEnhancer and Network Annotation Propagation

Wei-Yu Zhou[a], Zi-Han Xi[a], Ning-Ning Du[a], Li Ye[a], Ming-Hao Jiang[a], Jin-Le Hao[b], Bin Lin[c], Guo-Dong Yao[a], Xiao-Xiao Huang[a,*], Shao-Jiang Song[a,*]

[a] *Key Laboratory of Computational Chemistry-Based Natural Antitumor Drug Research & Development, Liaoning Province, Engineering Research Center of Natural Medicine Active Molecule Research & Development, Liaoning Province, Key Laboratory of Natural Bioactive Compounds Discovery & Modification, Shenyang, School of Traditional Chinese Materia Medica, Shenyang Pharmaceutical University, Shenyang 110016, China*
[b] *Key Laboratory of Structure-Based Drug Design and Discovery of Ministry of Education, Shenyang Pharmaceutical University, Shenyang 110016, China*
[c] *Wuya College of Innovation, Shenyang Pharmaceutical University, Shenyang 110016, China*

ARTICLE INFO

Article history:
Received 28 June 2023
Revised 29 August 2023
Accepted 30 August 2023
Available online 3 September 2023

Keywords:
Daphne altaica Pall.
Molecular networking
MolNetEnhancer
NAP
Unprecedented meroterpenoid frameworks
Neuroprotective activities
Acetylcholinesterase inhibitors

ABSTRACT

Under the guidance of the approach which integrates molecular networking, MolNetEnhancer and Network Annotation Propagation (NAP), daphnaltaicanoids A and B (**1** and **2**) with unprecedented 9-oxatetracyclo[6.6.1.0^{2,6}.0^{8,13}]pentadecane and tetracyclo[5.3.0.1^{2,5}.2^{4,11}]tridecane central frameworks were isolated from *Daphne altaica* Pall., representing two types of unparalleled meroterpenoid cores. Their structures were elucidated by extensive spectroscopic analysis, nuclear magnetic resonance (NMR) calculations, DP4+ analysis and electronic circular dichroism (ECD) calculations. The plausible biosynthetic pathways for **1** and **2** were postulated. Biologically, **2** exerted potent neuroprotective activities which were superior to trolox at 12.5 and 25 μmol/L. Moreover, **1** and **2** exhibited more noticeable acetylcholinesterase inhibitory activities than donepezil. Molecular docking simulations were performed to explore the intermolecular interaction of compounds **1** and **2** with acetylcholinesterase. The bioactivity evaluation results highlight the prospects of **1** and **2** as a novel category of neurological agents.

Natural products with novel skeletons usually contain complex fused rings and multiple stereogenic centers [1–4]. Due to their unique structures, they exhibit remarkable biological activities and have been recognized as fruitful resources for new drug seeds [5–8]. However, such compounds usually occur in the plant of origin at very low concentration levels. It is difficult to isolate them from complex mixtures using merely conventional repeated column chromatography [9]. Therefore, target isolation is urgently required to accelerate the research on compounds with novel skeletons.

Tandem mass spectrometry (MS/MS) molecular networking, which is publicly available *via* the Global Natural Products Social molecular networking (GNPS) web platform, has emerged as an efficient strategy that can facilitate the identification of low-abundant bioactive natural products with specific structural features [10–14]. But only finite number of nodes can be annotated owing to the limitation of the quantity of MS/MS spectra in available reference GNPS spectral libraries [15]. Accordingly, several advanced strategies have been designed to tackle the challenge in extending structural and chemical class annotations to molecules without any reference spectra deposited in public databases [16]. The MolNetEnhancer is one of the aforementioned tools which furnishes the chemical class annotations within molecular families and enhances chemical interpretations for unknown compounds [17]. The other online molecular network analysis tool named Network Annotation Propagation (NAP) can afford structural annotations by reranking of candidates even when there are no experimental library matches [18,19].

Our group focused on identifying structurally unique compounds from the genus *Daphne* and three guaiane-type sesquiterpenoids possessing complex caged systems and spiro-fused ring skeletons have been isolated from *Daphne penicillata* before [20–23]. In our continuous investigation for the compounds with fascinating architectures in the genus *Daphne*, a medicinal plant *Daphne altaica* Pall. (*D. altaica*) which was rarely reported came into our sight. Based on the preliminary MS/MS data, *D. al-*

* Corresponding authors.
E-mail addresses: xiaoxiao270@163.com (X.-X. Huang), songsj99@163.com (S.-J. Song).

https://doi.org/10.1016/j.cclet.2023.109030
1001-8417/

taica was inferred to contain meroterpenoids. Thus, we applied an approach which combines molecular networking, MolNetEnhancer and NAP together to achieve the target of seeking out compelling meroterpenoids efficiently and rapidly. On the basis of chemical class and framework annotations afforded by MolNetEnhancer, the molecular family which was predicted to comprise meroterpenoids was taken precedence to be isolated. Given the results of *in silico* top 10 ranked candidates through a consensus scoring algorithm in NAP, several specific nodes that were potentially assumed to possess complex meroterpenoid were prioritized from the selected molecular family. Guided by this approach, compounds **1** and **2** which featured unprecedented 9-oxa-tetracyclo[6.6.1.$0^{2,6}$.$0^{8,13}$]pentadecane and tetracyclo[5.3.0.$1^{2,5}$.$2^{4,11}$]tridecane central frameworks were identified from *D. altaica*, representing two types of unique highly cyclized meroterpenoid skeletons. Herein, the guided isolation, structural elucidation, plausible biosynthetic pathways and biological evaluation were described in depth.

The fraction A1 from *D. altaica* was analyzed by LC-MS/MS to prioritize the identification of fascinating meroterpenoids. The required data were processed following the molecular networking workflow on the GNPS platform and the analogous spectra were clustered as molecular families in the visualized version [24,25]. To further realize the putative chemical classification of molecular families and search for the molecular families which owned subtle substructural information related to meroterpenoids, the MolNetEnhancer workflow was applied. Meroterpenoids are hybrid natural products that comprise terpenoid and non-terpenoid parts like aromatic or indole fragment, *etc*. [26,27]. The generated MolNetEnhancer networks furnish information about the chemical class and framework of compounds in the CF_class and CF_Mframework terms, respectively. As revealed by Fig. 1, the molecular family A possessed the chemical class annotation of "prenol lipids" and framework annotation of "aromatic heteropolycyclic compounds", which represents the structures of the nodes in molecular family A might imply both terpenoid portion and aromatic part. Thus, based on the result analyzed by MolNetEnhancer, the molecular family A that were assumed to contain meroterpenoids could be selected for further separation.

The molecular family A contained 50 nodes and most of them were not annotated by GNPS MS/MS spectral library matching. In order to annotate the specific predicted structures of the nodes without any spectral library matching and explore the nodes which were possibly to possess complex meroterpenoid structures, the *in silico* annotation tool NAP was utilized in this molecular family. The *in silico* annotation tool NAP is conducted through creating a network consensus of re-ranked structural candidates using the molecular network topology and structural similarity, so that structural annotations could be applied even when there is no match to a MS/MS spectrum in spectral libraries. The *in silico* annotation tool NAP ranked 10 best candidates for each node in the molecular family A based on the consensus scores. We manually examined the structures of top 10 ranked candidates for each node in the molecular family A and found that the NAP consensus top 10 ranked candidates of five nodes with red borders in the molecular family A contained meroterpenoids with complex structures (Figs. S1–S5 in Supporting information). The precursor ion *m/z* values of these five nodes with red borders in Fig. 2 were 504.312, 539.316, 539.272, 539.271 and 539.269. The direct neighbor nodes tend to enjoy MS/MS spectra with the highest similarity in the molecular network. Hence, the aforementioned five nodes and the nodes directly connected to these five nodes were potentially predicted to possess complex meroterpenoid structures. The *in silico* annotation of NAP inspired us to focus on the isolation of these nodes. The application of molecular networking coupled to MolNetEnhancer and NAP led to the identification of compounds **1** and **2**, two meroterpenoids with two types of unparalleled skeletons (Fig. 3A).

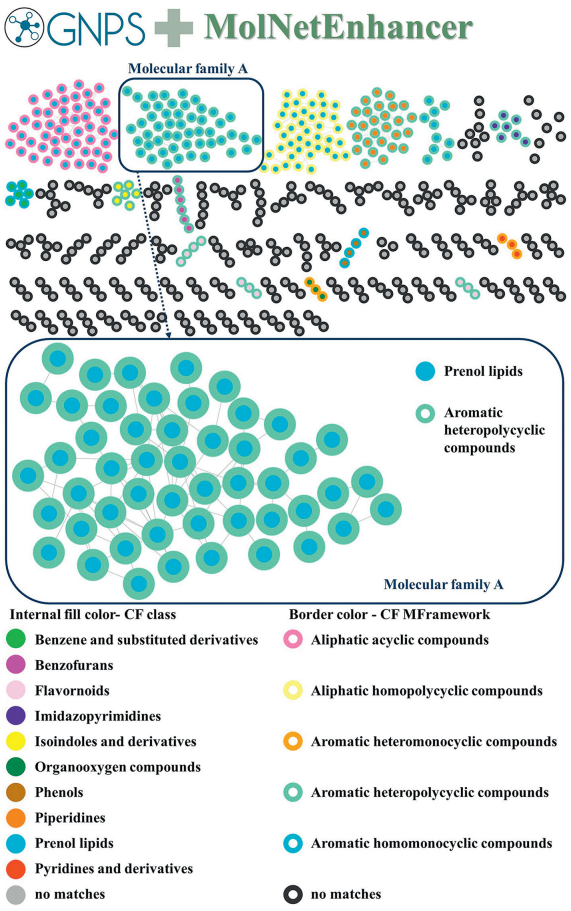

Fig. 1. The diagram of the combination of molecular networking and MolNetEnhancer towards the fraction A1 of *D. altaica*. Automatic classification and visualization of each cluster by the MolNetEnhancer. The internal fill colors and border colors of the nodes represent CF_class and CF_Mframework, respectively. The molecular family A with the chemical class annotation of "prenol lipids" and framework annotation of "aromatic heteropolycyclic compounds" (with the fill color of blue and the border color of bright green) were predicted to contain meroterpenoids. The almost singleton nodes were excluded in this figure.

Daphnaltaicanoid A (**1**) was determined to possess the molecular formula $C_{32}H_{34}O_5$ by using HRESIMS (*m/z* 499.2482 $[M + H]^+$, calcd. 499.2479), requiring 16 degrees of unsaturation. The ^{1}H nuclear magnetic resonance (NMR) spectroscopic data (Table S1 in Supporting information) of **1** displayed resonances corresponding to two monosubstituted phenyls [δ_H 7.85 (2H, m, H-19, H-23), 7.03 (2H, o, H-20, H-22), 7.10 (1H, m, H-21), 7.03 (2H, o, H-26, H-30), 7.08 (2H, m, H-27, H-29), 6.99 (1H, m, H-28)], two methyls [δ_H 0.81 (3H, s, H_3–31), 0.54 (3H, d, J = 6.9 Hz, H_3–32)] and a olefinic proton [δ_H 6.04 (1H, s, H-14)]. The ^{13}C NMR (Table S1) and heteronuclear singular quantum correlation (HSQC) data revealed the presence of 32 carbon signals, which were classified as two ketone carbonyls, one ester carbonyl, 12 benzene carbons, two olefinic carbons, two methyls, seven methylenes, two sp^3 methines and four sp^3 quaternary carbons.

The planar structure of **1** was established by extensive analysis of the 2D NMR spectroscopic data. In the heteronuclear multiple bond correlation (HMBC) spectrum (Fig. 3B), the correlations from H_3–32 to C-3 and C-5, from H-3 to C-1 and C-5 and from H-2 to C-4 deduced the existence of ring A. The presence of ring B was indicated from the HMBC correlations from H-6 to C-1, C-4, C-11, from H_3–31 to C-1 and from H-2 to C-10. The HMBC corre-

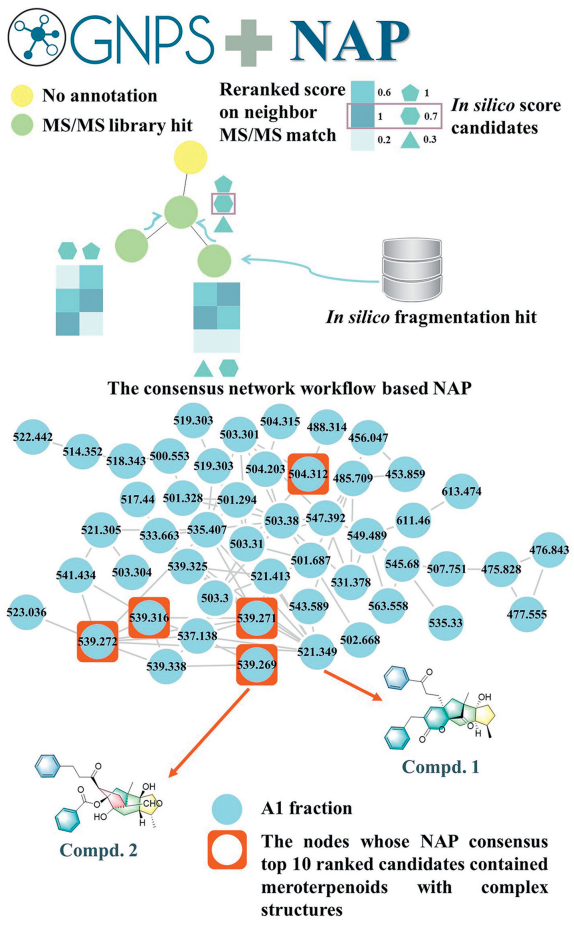

Fig. 2. The diagram of the combination of molecular networking and NAP towards the molecular family A of fraction A1 from *D. altaica*. Targeted isolation of the nodes which were assumed to be meroterpenoids within the selected molecular family (molecular family A) using NAP. NAP analyzed all nodes in the molecular family A and the NAP consensus top 10 ranked candidates of five nodes with red borders contained meroterpenoids with complex structures.

lations from H_3–31 to C-9 and C-11, from H-9 to C-1, C-7 and C-11 and from H-6 to C-8 allowed the construction of ring C which was fused to ring B through a bridged carbon bond of C10-C11-C-7. The ring D was linked to ring C at C7/C8, as verified by the downfield shifting of C-7 (δ_C 88.1) and the HMBC correlations from H-14 to C-7, C-12 and C-9. The esterification position of **1** was further proved by analyzing the obtained spectroscopic data using computer-assisted structure elucidation software (ACD/Spectrus Processor) [28,29]. By comparing the ^{13}C spectrum data with predicted ^{13}C NMR chemical shifts of possible candidates **1A** (esterification at 7-OH) and **1B** (esterification at 1-OH), **1A** with the highest match factor (MF) value (0.92) and the lowest standard deviation values [d_N (^{13}C) of 1.936 and sd_N (^{13}C) of 2.920] was verified as the most reasonable structure (Fig. S6 in Supporting information). Thus, the unit A of **1** was elucidated as a unique 9-oxatetracyclo[6.6.1.$0^{2,6}$.$0^{8,13}$]pentadecane skeleton featuring a unique 5/6/5/6 ring system. The HMBC correlations of H-15 with C-9, C-14, C-7 and C-17, H-16 with C-8, H-19 and H-23 with C-21, H-19 with C-23 and H-19 and H-23 with C-17 revealed the presence of unit B which was connected to unit A at C-8. Furthermore, the existence of unit C and its attachment to the C-13 of unit A were inferred from the HMBC correlations of H-26 and H-30 with C-28, H-26 to C-30, H-24 to C-26 and C-30, H-14 to C-24 and H-24 to C-12. Therefore, the planar structure of **1** was unequivocally established.

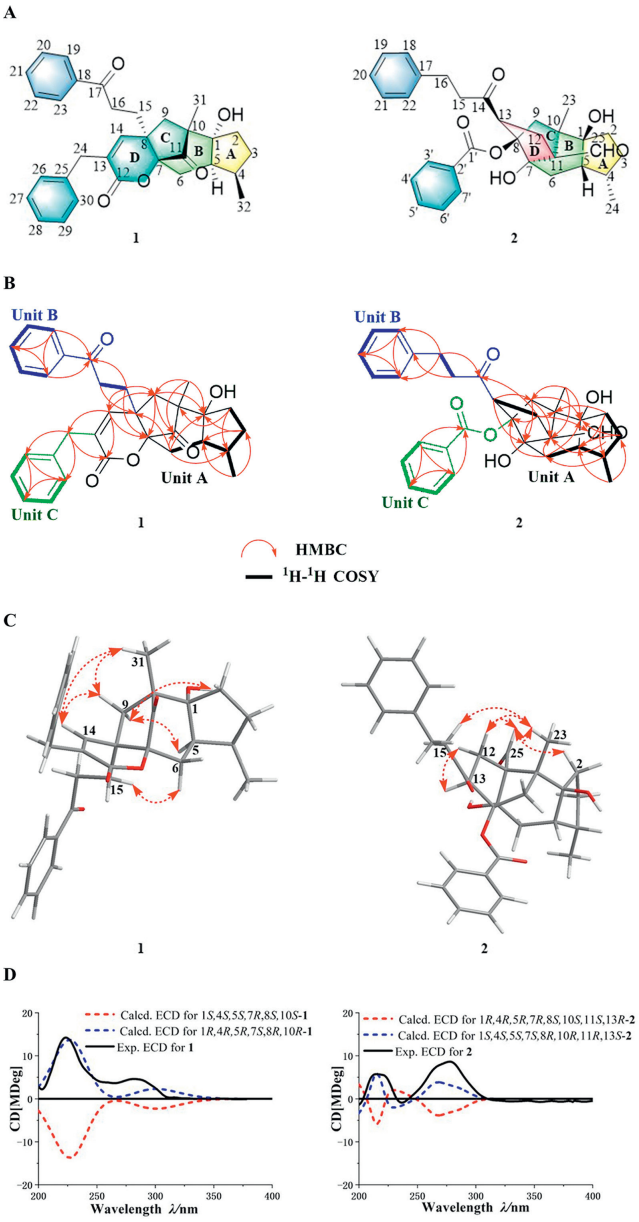

Fig. 3. (A) Chemical structures of compounds **1** and **2**. (B) Key HMBC and ^{1}H-^{1}H COSY correlations for **1** and **2**. (C) Key NOESY correlations for **1** and **2**. (D) Experimental and calculated ECD spectra for **1** and **2**.

The relative configuration of **1** was partially assigned through the nuclear overhauser effect spectroscopy (NOESY) correlations (Fig. 3C). Based on the NOESY interactions between H-5 and H-9α, H-9β and H_3–31, H-9β and H-14, H-14 and H_3–31, H-9α and 1-OH, H-15 and H-6α, the relative configuration was partially assigned as 1*R**,5*R**,7*S**,8*R**,10*R**. The quantum chemical calculations of ^{13}C NMR chemical shifts with DP4+ analysis was further used to determine the relative configuration of C-4 of **1**. Two reasonable diastereomers, (1*R**,4*S**,5*R**,7*S**,8*R**,10*R**)–**1** (**1–1**) and (1*R**,4*R**,5*R**,7*S**,8*R**,10*R**)–**1** (**1–2**), were conducted to NMR chemical shift calculations using the gauge independent atomic orbital (GIAO) method at the mPW1PW91/6–311+G(d,p) level. The computed ^{13}C NMR chemical shifts of **1–2** corresponded well to the experimental data with the DP4+ probability of 100.00% (99.69% for ^1H and 100.00% for ^{13}C) and the corrected mean absolute errors (CMAE) of 2.11, defining the relative configuration of **1** as (1*R**,4*R**,5*R**,7*S**,8*R**,10*R**)–**1** (**1–2**) (Fig. S7 in Supporting informa-

tion). The absolute configurations of **1** could be deduced from time-dependent density functional theory (TDDFT)/ECD calculations. The ECD curves generated for (1*R*,4*R*,5*R*,7*S*,8*R*,10*R*)−**1** agreed well with the experimental curves for **1**, allowing the assignment of the absolute configuration of **1** as 1*R*,4*R*,5*R*,7*S*,8*R*,10*R* (Fig. 3D).

The molecular formula of daphnaltaicanoid B (**2**) was established as $C_{32}H_{36}O_6$ on the basis of the HRESIMS ion peak at *m/z* 517.2586 $[M + H]^+$ (calcd. for $C_{32}H_{37}O_6$, 517.2585), indicating 15 indices of hydrogen deficiency. The ^{1}H NMR spectrum (Table S1) exhibited signals assignable to two sets of monosubstituted phenyls [δ_H 7.10 (2H, o, H-18, H-22), 7.10 (2H, o, H-19, H-21), 7.01 (1H, o, H-20), 8.15 (2H, m, H-3′, H-7′), 7.01 (2H, o, H-4′, H-6′), 7.08 (1H, m, H-5′)], two methyls [δ_H 1.22 (3H, s, H_3–23), 0.60 (3H, d, J = 6.9 Hz, H_3–24)], one formyl group [δ_H 9.71 (1H, s, 25-CHO)]. The ^{13}C NMR data (Table S1) in conjunction with HSQC spectrum revealed the existence of 32 carbons, which were ascribed to one ketone carbonyl, one formyl, one ester carbonyl, two monosubstituted benzene rings, two methyls, seven methylenes, three methines, five sp^3 hybridized quaternary carbons.

The HMBC correlations (Fig. 3B) from H_3–24 to C-3 and C-5, from H-3 to C-1 and C-5 and from H-2 to C-4 and C-5 evidenced the existence of ring A. The presence of ring B was validated by HMBC cross signals from H-4 to C-6, from H-2 to C-10, from H_3–23 to C-1 and C-11, from H-6 to C-11 and C-1, along with the ^{1}H-^{1}H correlation spectroscopy (COSY) correlation of H-5/H-6. The HMBC correlations of H-9 with C-11, C-7 and C-1, H-6 with C-8 and H_3–23 with C-9 confirmed the presence of a five-membered ring (ring C) fused with ring B through the C10-C11-C7 bond. The HMBC interactions from H-12 with C-10, C-7 and C-8 and H-13 with C-9 and C-7, in combination with the ^{1}H-^{1}H COSY correlation of H-12/H-13 revealed the existence of ring D and indicated ring D was fused to ring C *via* C8-C7-C11 linkage. The assignment of the formyl group at C-11 was evidenced from the HMBC correlation from 25-CHO to C-11. Thus, the unit A of **2** was constructed as an unprecedented caged tetracyclo[5.3.0.1^{2,5}.2^{4,11}]tridecane core with 5/6/5/5 ring system. The HMBC correlations from H-12 to C-14, from H-15 to C-17, from H-16 to C-18, C-22 and C-14, from H-18 and H-22 to C-20, from H-18 to C-22, together with the ^{1}H-^{1}H COSY correlations of H-15/H-16 and H-18/H-19/H-20/H-21/H-22 verified the presence of unit B and its linkage to C-13 of unit A. The occurrence of unit C was corroborated by the HMBC correlations of H-3′ and H-7′ with C-1′, H-3′ and H-7′ with C-5′, and H-3′ with C-7′ as well as the ^{1}H-^{1}H COSY correlation of H-3′/H-4′/H-5′/H-6′/H-7′. Moreover, unit C was implied to link to the C-8 of unit A due to the significant downfield chemical shift of C-8 (δ_C 98.5). This was further confirmed using the ACD/Spectrus Processor. By comparing the ^{13}C spectrum data with predicted ^{13}C NMR chemical shifts of possible candidates **2A** (esterification at 8-OH), **2B** (esterification at 7-OH) and **2C** (esterification at 1-OH), **2A** with the highest MF value (0.94) and the lowest standard deviation values [d_N (^{13}C) of 2.058 and sd_N (^{13}C) of 2.583] was validated as the most reasonable structure (Fig. S8 in Supporting information). The planar structure of **2** was thus delineated as depicted.

The NOESY correlations (Fig. 3C) of 25-CHO/H_3–23, H_3–23/H-12β, H-12β/25-CHO, H-12α/H-13, H-15/H_3–23 and 25-CHO/H-2α ascertained the partial relative configuration as 1*S**,7*S**,8*R**,10*R**,11*R**,13*S**. To determine the configuration of C-4 and C-5, the ^{13}C chemical shifts of four possible isomers (1*S**,4*S**,5*R**,7*S**,8*R**,10*R**,11*R**,13*S**)−**2** (**2–1**), (1*S**,4*R**,5*R**,7*S**,8*R**,10*R**,11*R**,13*S**)−**2** (**2–2**), (1*S**,4*S**,5*S**,7*S**,8*R**,10*R**,11*R**,13*S**)−**2** (**2–3**) and (1*S**,4*R**,5*S**,7*S**,8*R**,10*R**,11*R**,13*S**)−**2** (**2–4**) were calculated and the (1*S**,4*S**,5*S**,7*S**,8*R**,10*R**,11*R**,13*S**)−**2** (**2–3**) matched well with the NMR experimental data with the DP4+ probability of 100.00% (98.98% for ^{1}H and 100.00% for ^{13}C) and the CMAE of 1.93 (Fig. S7). Additionally, the ECD calculation for the (1*S*,4*S*,5*S*,7*S*,8*R*,10*R*,11*R*,13*S*) structure was then conducted and the results were consistent with the experimental spectrum, establishing the absolute configuration of **2** as (1*S*,4*S*,5*S*,7*S*,8*R*,10*R*,11*R*,13*S*) (Fig. 3D).

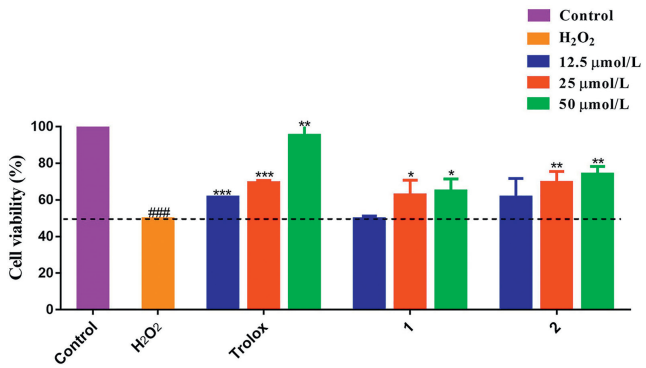

Fig. 4. Neuroprotective effects of **1** and **2** against H_2O_2-induced injury in SH-SY5Y cells. Data (cell viability) were presented as means ± standard error of mean (SEM). $^*P < 0.05$, $^{**}P < 0.01$, $^{***}P < 0.001$ *vs.* H_2O_2 group; $^{\#\#\#}P < 0.001$ *vs.* control group.

Structurally, two meroterpenoids daphnaltaicanoids A (**1**) and B (**2**) are the first hybrid examples of two sets of aromatic derivatives and sesquiterpenoids featuring two types of unprecedented 9-oxa-tetracyclo[6.6.1.0^{2,6}.0^{8,13}]pentadecane and tetracyclo[5.3.0.1^{2,5}.2^{4,11}]tridecane skeletons, respectively. The biosynthetic pathways of **1** and **2** (Scheme S1 in Supporting information) could be traced back to the precursors, wikstronone A and wikstronone C [21], respectively, two major guaiane-type sesquiterpenoids of *D. altaica*, which had been isolated by us in genus *Daphne* before. Wikstronone A underwent several steps including isomerization, hydrogenation, hydration, oxidation, dehydration, decarbonation, dehydrogenation, electrocyclic reactions to generate intermediate h [30–32]. Subsequently, intermediate h would be converted intermediate l through oxidative cleavage, oxidation, protonation, hydrogenation, C10-C11 cyclization reactions. The Michael addition of intermediate l with 1-phenylprop-2-en-1-one gave rise to intermediate m which possessed the 5/6/5 ring system. Through the esterification of intermediate m and 3-phenylpropanoic acid, the ester carbonyl bond at C-12 was formed. Then, the Aldol condensation and dehydration reactions of intermediate n established the connectivity of C-13-C-14 to construct ring D, thus compound **1** with distinctive 9-oxa-tetracyclo[6.6.1.0^{2,6}.0^{8,13}]pentadecane core was formed. Wikstronone C underwent isomerization, hydrogenation, hydration, oxidation, demethylation, protonation and C10-C11 cyclization reactions to form intermediate t. Intermediate t underwent Michael addition with 5-phenylpent-1-en-3-one to acquire intermediate u. The connection of C-8 and C-13 was furnished by the Aldol condensation of intermediate u, which led to the formation of intermediate v with unexpected tetracyclo[5.3.0.1^{2,5}.2^{4,11}]tridecane core. Further esterification with benzoic acid accomplished the ester carbonyl bond at C-1′, resulting in the appearance of compound **2**.

Compounds **1** and **2** were examined for their neuroprotective activities against SH-SY5Y cell damage induced by H_2O_2 using MTT assay and trolox was assigned as positive control [33,34]. As revealed in Fig. 4, treatment of H_2O_2 reduced the viability of SH-SY5Y cells to 49.69%, compared with the control group. The results demonstrated that **2** exerted potent neuroprotective activities with cell viabilities of 61.65% and 69.63% at 12.5 and 25 μmol/L, respectively, which were both superior to trolox at the same concentration (61.59% at 12.5 μmol/L and 69.42% at 25 μmol/L). These compounds were also evaluated for their acetylcholinesterase (AChE) inhibitory activities. Donepezil was used as positive control [35–37]. Compounds **1** and **2** exhibited remarkable AChE inhibitory activities with half maximal inhibitory concentration (IC_{50}) values of

0.02 ± 0.02 and 0.31 ± 0.18 μmol/L, which were more significant than donepezil (IC_{50}: 1.85 ± 0.03 μmol/L). The molecular docking analysis of **1** and **2** was implemented to better investigate the putative binding mode of them with AChE (Fig. S9 in Supporting information). The 12-CO of **1** interacted with amino acid residue PHE 288 of AChE through hydrogen bond. Compound **1** could also form two π-π stacking interactions with TRP 279 and TYR 334 at two benzene rings. The 1-OH and 7-OH of **2** could form two hydrogen bonds with TRP 279 and ASP 285 of AChE, respectively. In addition, one phenyl ring of **2** bonded with TRP 279 through π-π stacking interaction. The result indicated that the potent AChE inhibitory activities of compounds **1** and **2** might arise from the hydrogen bonds and π-π stacking interactions.

In summary, we applied the approach by integration of molecular networking, MolNetEnhancer and NAP to search for bioactive meroterpenoids with intriguing architectures from *D. altaica*. Guided by this approach, daphnaltaicanoids A and B (**1** and **2**) possessing unprecedented 9-oxa-tetracyclo[6.6.1.$0^{2,6}$.$0^{8,13}$]pentadecane and tetracyclo[5.3.0.$1^{2,5}$.$2^{4,11}$]tridecane central frameworks were identified, representing two categories of unparalleled meroterpenoid cores. This successful investigation demonstrates the high potential of rapidly finding novel skeleton natural products through the combination of molecular networking, MolNetEnhancer and NAP. Results of bioactivity study showed that compound **2** exerted potent neuroprotective activities which were superior to trolox at 12.5 and 25 μmol/L. Moreover, **1** and **2** exhibited more remarkable acetylcholinesterase inhibitory activities than donepezil. Considering the structural novelty and potential therapeutic value of **1** and **2**, the current study not only enriches the chemical diversity of meroterpenoids, but also furnishes new chemical scaffolds for developing novel neurological agents.

Declaration of competing interest

The authors declare that they have no known competing financial interests or personal relationships that could have appeared to influence the work reported in this paper.

Acknowledgments

The work was financially supported by the National Natural Science Foundation of China (Nos. 82073736, 81872766), Science and Technology Planning Project of Liaoning Province (No. 2021JH1/10400049) and Liaoning revitalization talents program (Nos. XLYC2002066, XLYC2007180).

Supplementary materials

Supplementary material associated with this article can be found, in the online version, at doi:10.1016/j.cclet.2023.109030.

References

[1] Y. Li, L. Zhang, W. Wang, et al., Bioorg. Chem. 128 (2022) 106106.
[2] J.J. Zhao, S.Z. Du, K. Hu, et al., Chin. Chem. Lett. 34 (2023) 107737.
[3] X.Y. Hu, X.M. Li, S.Q. Yang, et al., Chin. Chem. Lett. 34 (2023) 107516.
[4] Y. Ding, Y. Jiang, S.J. Xu, X.J. Xin, F.L. An, Chin. Chem. Lett. 34 (2023) 107562.
[5] R. Taguchi, A. Iwasaki, A. Ebihara, et al., Org. Lett. 24 (2022) 4710–4714.
[6] J.H. Ye, G.Y. Luo, C.L. Zhao, et al., Chin. Chem. Lett. 34 (2023) 108621.
[7] Y.Y. Feng, S.Q. Zha, H.Q. Zhang, et al., Chin. Chem. Lett. 34 (2023) 107742.
[8] S.S. Chen, H.X. Liu, S.N. Li, et al., Chin. Chem. Lett. 34 (2023) 107513.
[9] V.F. Freire, J.R. Gubiani, T.M. Spencer, et al., J. Nat. Prod. 85 (2022) 1340–1350.
[10] G. Cauchie, E.O. N'Nang, J.J.J. van der Hooft, et al., Org. Lett. 22 (2020) 6077–6081.
[11] J.X. Li, Z.R. Cui, Y.Y. Li, et al., Chin. Chem. Lett. 33 (2022) 4257–4260.
[12] S. Lin, J.Z. Huang, H.X. Zeng, et al., Chin. Chem. Lett. 33 (2022) 4587–4594.
[13] H. Gu, G.X. Dai, S.Y. Liu, et al., Chin. Chem. Lett. 34 (2023) 107715.
[14] J.Y. Zhang, F. Liu, Q. Jin, et al., Chin. Chem. Lett. 35 (2024) 108881.
[15] A.E. Fox Ramos, C. Pavesi, M. Litaudon, et al., Anal. Chem. 91 (2019) 11247–11252.
[16] M.A. Beniddir, K.B. Kang, G. Genta-Jouve, et al., Nat. Prod. Rep. 38 (2021) 1967–1993.
[17] M. Ernst, K.B. Kang, A.M. Caraballo-Rodríguez, et al., Metabolites 9 (2019) 144.
[18] R.R. da Silva, M.X. Wang, L.F. Nothias, et al., PLoS Comput. Biol. 14 (2018) e1006089.
[19] K.B. Kang, E.J. Park, R.R. da Silva, et al., J. Nat. Prod. 81 (2018) 1819–1828.
[20] P. Zhao, Z.Y. Li, S.Y. Qin, et al., J. Org. Chem. 86 (2021) 15298–15306.
[21] W.Y. Zhou, J.Y. Hou, Q. Li, et al., Phytochemistry 204 (2022) 113468.
[22] S.H. Dong, Z.K. Duan, Y.F. Ai, et al., Bioorg. Chem. 129 (2022) 106208.
[23] S.H. Mi, P. Zhao, Q. Li, et al., Phytochemistry 198 (2022) 113144.
[24] Z.H. Chen, D.D. Yu, C. Li, et al., Chemistry 29 (2023) e202203487.
[25] W.Y. Zhou, J.Q. Niu, Q. Li, et al., J. Agric. Food. Chem. 71 (2023) 3338–3349.
[26] R. Geris, T.J. Simpson, Nat. Prod. Rep. 26 (2009) 1063–1094.
[27] H.W. Yan, R.R. Du, X. Zhang, et al., Chin. Chem. Lett. 33 (2022) 2555–2558.
[28] C.L. Xie, D. Zhang, K.Q. Guo, et al., Chin. Chem. Lett. 33 (2022) 2057–2059.
[29] T.M. Lv, D.L. Chen, J.J. Liang, et al., Org. Lett. 23 (2021) 7231–7235.
[30] J.J. Liang, T.M. Lv, Z.Y. Xu, et al., Fitoterapia 165 (2023) 105400.
[31] X. Wang, F.J. Liu, T. Xu, Chin. Chem. Lett. 34 (2023) 107624.
[32] P.Y. Yang, Q. Jia, S.J. Song, X.X. Huang, Nat. Prod. Rep. 40 (2023) 1094–1129.
[33] X.L. Qi, Y.Y. Zhang, P. Zhao, et al., J. Nat. Prod. 81 (2018) 1225–1234.
[34] Q. Ren, W.Y. Zhao, S.C. Shi, et al., J. Nat. Prod. 82 (2019) 1510–1517.
[35] Y.L. Liu, G. Uras, I. Onuwaje, et al., Eur. J. Med. Chem. 235 (2022) 114305.
[36] X.Y. Jiang, C. Liu, M.X. Zou, et al., Eur. J. Med. Chem. 223 (2021) 113663.
[37] P. Wang, Y. Wang, P. Li, et al., Chin. Chem. Lett. 34 (2023) 107691.